Trans Indian Inst Met (2022) 75(4):949–957
https://doi.org/10.1007/s12666-022-02533-5

ORIGINAL ARTICLE

Theoretical investigations on the evolution of ordering in Ni–Mo-based alloys

Rumu H. Banerjee[1,2] · A. Arya[2,3] · H. Donthula[1,2] · R. Tewari[1,2]

Received: 27 October 2021 / Accepted: 16 January 2022 / Published online: 17 February 2022
© The Indian Institute of Metals - IIM 2022

Abstract The competing ordering and clustering tendencies in Ni–Mo alloy system are manifested by having nearly equal stabilities of superlattice structures whose enthalpies are dictated by interaction energies between near neighbours in different coordination shells. These effective cluster interaction parameters (ECIs) dictate the complex ordering/clustering processes. In the present investigation, the evolution of $D1_a$ structure of Ni_4Mo from the < 1 0 > short-range ordered structure in the fcc matrix of same composition was studied using electron microscopy. Cluster expansion formalism in conjunction with density functional theory-based calculations was employed to determine the ECIs for the alloy. It was concluded that pair, triplet and quadruplet ECIs stabilize unlike atoms in the first coordination. Finally, it was shown that these ECIs could be used with reasonable accuracy in the Monte Carlo simulations to evaluate Gibbs free energies of formation as a function of temperature, short- and long-range-order parameters to understand ordering/clustering tendencies and hence transformation pathways in the alloy.

Keywords Ni–Mo alloys · Order–disorder transformations · Intermetallic alloys and compounds · Simulation and modelling · Cluster expansion

✉ Rumu H. Banerjee
rumuhalder24feb@gmail.com

[1] Materials Science Division, Bhabha Atomic Research Centre, Mumbai 400 085, India

[2] Homi Bhabha National Institute, Mumbai 400 094, India

[3] Glass and Advanced Materials Division, Bhabha Atomic Research Centre, Mumbai 400 085, India

1 Introduction

Ordered intermetallics are ubiquitously formed in the microstructures of several Ni-based superalloys such as Hastelloys, Inconels, etc., upon prolonged exposure at elevated temperatures (973–1273 K) [1, 2]. These Ni–Mo and Ni–Cr based alloys undergo order–disorder phase transitions leading to the development of face-centred cubic (fcc) based long-range ordered (LRO) precipitates, e.g. Pt_2Mo-type, $D0_{22}$, $L1_2$, $D1_a$, etc., [1, 2] and remain coherent with the disordered fcc alloy matrix. These LRO precipitates lead to significant lattice dimensional changes and stresses which result in altered mechanical properties such as reduced ductility, enhanced strength, negative creep [2–4] and, therefore, play a decisive role in predicting the service life of the alloys at operating temperatures.

Of the several ordering phase transformations possible in Ni-based alloys, the most extensively investigated system is the Ni–Mo system [5–9] with Mo concentration varying between 8 and 33 at.%. The as-quenched structure of Ni–Mo alloy shows a short wave length concentration modulated structure described by wave vector, $k = < 1\ ½\ 0 >$ [4–7] within a fcc matrix. Upon ageing, these binary alloys show order–disorder phase transformation featuring several competing stable and metastable face-centred cubic (fcc) superlattice structures, such as $D1_a$ (Ni_4Mo), stable $D0_a$ (Ni_3Mo), metastable $D0_{22}$ (Ni_3Mo) and Pt_2Mo (Ni_2Mo) type configurations. The $D0_{22}$ (Ni_3Mo) phase forms only with ternary additions and for ageing temperatures below 900 K. The formation of various fcc-based superstructures at different Mo concentrations is summarized in schematic presented in Fig. 1 [4–8]. The relative stabilities and transformation sequence of these competing structures are governed by the underlying ordering and clustering tendencies present in the system dictated by

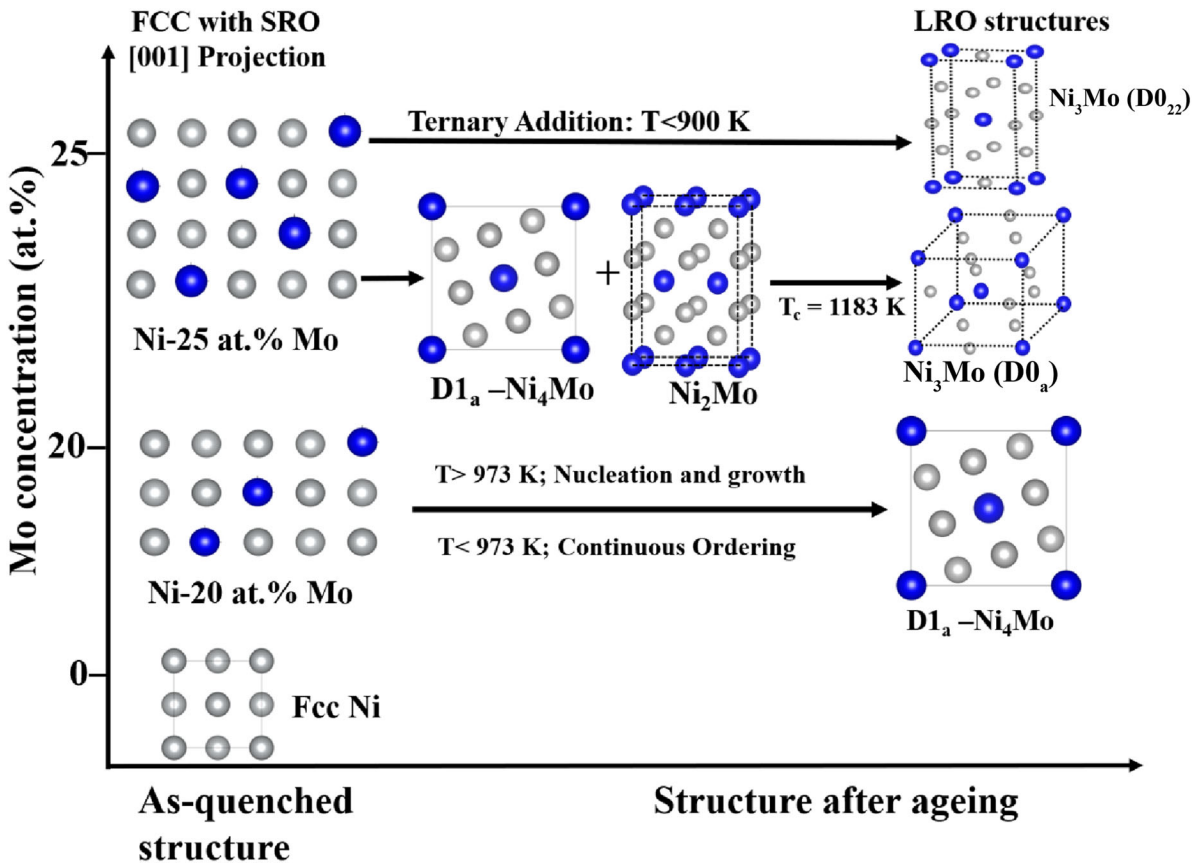

Fig. 1 Schematic showing the ordering transformations in Ni–Mo system (Mo: 0–25 at%). Ni and Mo atoms are shown as grey and blue circles, respectively

nearest neighbour (NN) configurations and their interaction energies [5–9]. Therefore, in order to understand the order–disorder phase transformation sequence, it is essential to have knowledge of pair and multisite interaction energies [9] and their role in altering the NN configurations with temperature. Earlier tight binding approximation and cluster variation methods were used to evaluate these interaction energies [9]. However, the cluster expansion (CE)-based approach [10] has emerged as a robust method to accurately determine the thermodynamics of an alloy in conjunction with the Monte Carlo method. The CE approach interfacing with any density functional theory (DFT) is used to evaluate the Gibbs free energy of any configuration as a function of short- and long-range-order parameters and temperature [9, 10].

In the present study, the evolution of $D1_a$ type (Body-centred tetragonal; I4/m) ordered precipitates in Ni-20 at.% Mo alloy (Ni_4Mo) was studied both experimentally and theoretically. A literature survey suggests that only a limited work has been carried out to evaluate the interaction parameters to study the order–disorder phase transformations [7–9, 11]. In earlier studies, the phase stability of different coherent superstructures was described mainly in terms of effective pair interaction parameters up to the fourth coordination shell and the configurational energy was evaluated using the tight binding-linear muffin tin orbital method (TB-LMTO); while the configurational entropy calculation was based on either static concentration wave (SCW) or cluster variation method (CVM) models [7–9]. In addition, the instability domains as a function of short and long wavelength concentration fluctuations could be identified from these calculations and the sequence of transformation could be predicted [4–12]. However, the role of multisite interactions, namely, triplet and quadruplet interactions, remained unexplored mostly due to the computational challenges associated with the cluster variation method.

Furthermore, the nature of SRO parameters and their variation with temperature also needs to be investigated to understand the initial < 1 ½0 > ordering in these alloys which is important to gain the insights on the transformation behaviour and correlate the transformation sequence with the microstructure and hence mechanical properties, such as hardness. The knowledge gained for the binary Ni–Mo system can be used to further extend the understanding of commercial Ni-based alloys such as Hastelloy N

(Cr + Mo = 20 at.%; ternary counterpart of Ni-20 at.% Mo alloy), Hastelloy C-22, [1–4] which are potential structural material for use in the advanced reactors [1–4, 13].

2 Materials and methods

2.1 Experimental methodology

The studied alloy having composition of Ni-20 at.% Mo was prepared by vacuum arc melting of Ni and Mo pieces which was then hot rolled at 1173 K. The alloy was subsequently solution annealed for 1 h at 1223 K in evacuated quartz capsules followed by water quenching. The chemical composition of the alloy was verified by X-ray fluorescence (XRF) and energy-dispersive spectroscopic (EDS) techniques (Table 1). The as-quenched alloy coupons were again sealed in evacuated quartz tubes and subjected to ageing treatments carried out at 873 K, 973 K and 1073 K for varying durations (2–50 h). Samples for TEM investigations were prepared by punching out 3 mm diameter discs from ~ 100-µm thick alloy foils. These discs were then polished in a twin jet electro-polishing unit using 90% methanol and 10% perchloric acid electrolytic bath maintained at 233 K. Bright field and dark field images were recorded in a JEOL 2000FX TEM operated at 160 kV. The high-resolution images were recorded in FEI TECHNAI TEM operated at 200 kV.

Microhardness measurements on the as-quenched and aged samples were made with a Vicker's microhardness tester by applying a constant load of 300 gf for a dwell time of 15 s. A total of 10 measurements at different locations on the polished alloy specimens were recorded, and the average value was calculated.

2.2 Cluster expansion-based approach

The 2-point (pair), 3-point (triplet) and 4-point (quadruplet) cluster interaction parameters (ECIs) were calculated using Alloy Theoretic Automated Toolkit (ATAT) package [13, 14] based on cluster expansion (CE) formalism. Under the CE framework, the Ising like Hamiltonian for any N-lattice site configuration of the alloy is described by a configuration variable σ_i defined for each lattice site i. The σ_i can take up values + 1(− 1) if the atomic species at site i is Ni (Mo). The configurational energy Hamiltonian of the alloy for any configuration σ is then expressed as [10, 13, 14]

$$E(\sigma) = \sum_{\beta} D_{\beta} J_{\beta} \prod_{i \in \beta'} \sigma_i \tag{1}$$

where J_β is the effective cluster (β) interaction coefficients (ECIs), D_β is the cluster degeneracy and $\langle \prod_{i \epsilon \alpha \beta'} \sigma_i \rangle$ describes different types of clusters (point, pair, triplets, etc.) correlation functions. The ground-state energies of several ordered structures were evaluated using DFT formalism as encapsulated in "Vienna Ab-initio Simulation Package (VASP)" [15] employing generalized gradient approximation with exchange–correlation functional as parameterized by Perdew–Burke–Ernzerhof (PBE) [16] and projector-augmented wave (PAW)-type pseudopotentials. High-quality k-point mesh up to 12 × 12x 12 grid under the Monkhost-Pack scheme was used for Brillouin zone sampling [17]. The energies of the ordered structures were fitted by generating suitable clusters through CE approach to evaluate the ECIs.

2.3 Evaluation of Warren Cowley parameters

The ordering tendency originates from the stronger attraction between unlike atoms as compared to like atoms. This preference for unlike atom in the first few neighbouring shells for a binary alloy $Ni_{1-c}Mo_c$ (c being Mo atom fraction) can further be quantified using Warren Cowley (WC) parameters. WC parameter for j^{th} coordination shell, α_j^{Ni-Mo}, is defined by following expression [18]

$$\alpha_j^{Ni-Mo} = 1 - \frac{P_j^{Ni-Mo}}{c} \tag{2}$$

where $c = 0.2$ is the Mo atom fraction, P_j^{Ni-Mo} is the probability of finding Ni around Mo at the jth coordination shell. The values of α_j were calculated for ordered Ni_4Mo phase with $D1_a$ structure at 300 K using the following expression [10]

Table 1 Composition of the alloy studied

Element	Theoretical composition		Experimental composition (wt%)	
	(at.%)	(wt.%)	EDS	XRF
Ni	80	70.5	70.8(± 0.1)	70.4(± 0.1)
Mo	20	29.5	29.2(± 0.1)	28.7 (± 0.1)

$$\alpha_j = \frac{\langle \pi \rangle - (2c-1)^2}{1-(2c-1)^2} \quad (3)$$

where $\langle \pi \rangle$ is the pair correlation defined in terms of configurational variables. The sign of α determines whether the atoms prefer to order ($\alpha < 0$) or cluster (> 0). The temperature dependence of α_l, for the *l*th coordination shell with vertices at lattice positions *n* and *n'*, is determined from the point (σ_n) and pair ($\sigma_n \sigma_{nn'}$) configurational variables as [10, 13]

$$\alpha_{nn'} = \frac{\langle \sigma_n \sigma_{n'} \rangle - \langle \sigma_n \rangle \langle \sigma_{n'} \rangle}{1 - \langle \sigma_n \rangle \langle \sigma_{n'} \rangle} \quad (4)$$

Once the ECIs are known, then standard statistical mechanics approach of Monte Carlo method (MC) can be applied to any configuration σ to determine the correlation functions for pair clusters as a function of temperature (T) using the expression [10, 13, 14, 19]

$$\langle \pi \rangle_T = \frac{\sum_\beta \pi(\sigma) e^{-E(\sigma)/K_b T}}{\sum_\beta e^{-E(\sigma)/K_b T}} \quad (5)$$

where $\langle \pi \rangle_T$ is the pair correlation function at temperature T, $E(\sigma)$ is the energy of the configuration σ and K_b is the Boltzmann constant (8.617×10^{-5} eV K^{-1}).

2.4 Determination of Gibbs free energy as a function of temperature

In this approach, the total free energy of the ensemble (*G*) is allowed to change under an externally specified T keeping the total number of atoms (*M*) fixed [10, 13]. The grand canonical potential Φ is obtained from the partition function (*Z*) which in turn is evaluated from the Metropolis algorithm incorporated in the MC approach. The grand canonical potential Φ is defined as [10, 14]

$$\Phi = \frac{-\ln Z}{MK_bT} = \frac{-1}{MK_bT} \ln\left(\sum_i \exp\left(-M\beta\left(E_j - \omega c_j\right)\right)\right) \quad (6)$$

where E_j is the formation energy of any configuration '*j*' obtained using the ECI values evaluated from the CE approach, c_j is the solute concentration at that configuration and K_b is the Boltzmann constant. The chemical potential, ω, is the chemical potential that stabilizes a two-phase equilibrium between ordered ($D1_a$) and disordered (fcc) Ni_4Mo. The sum extends to all the states possible for the system.

Modelling of the order–disorder phase transformations in Ni-20 at.% Mo was carried out by the Easy Monte Carlo Code (EMC2) module of ATAT. MC simulations were performed on supercell made by 25 × 25 × 25 expansion of the unit cell in the temperature range 400–1200 K while specifying ω. The change in configuration was achieved by changing the Mo and Ni occupied sites and accepting the flip on the basis of Metropolis algorithm. Detailed algorithm of EMC2 is provided in refs. [10, 14].

3 Results and discussion

3.1 Experimental study

3.1.1 Electron microscopic investigations

The specimens of Ni-20 at.% Mo alloy under as-quenched as well as heat treated at 873 K for 2 h conditions show a single phase matrix in the bright field (Fig. 2a–b), but the presence of diffused intensities at (1 ½ 0) positions and complete absence of (210) reflections in the SAED patterns indicate the presence of a short-range ordering (SRO) in the alloy (Fig. 2c)). These SROs in Ni-20 at.% Mo are explained at length by Arya et al. [2, 3, 9], Banerjee et al.[5] and Hata et al. [7, 8].

Ni-20 at.% Mo alloy, after ageing at 973 K-1073 K for 4 h-50 h, reveals formation of weak spots at $\frac{1}{5}\{4\ 2\ 0\}$ positions and complete disappearance of {1 ½ 0} in the [001] SAED pattern indicating the initiation of formation of the ordering domains of $D1_a$ structure as shown in Fig. 2d–f. These additional superlattice spots at $\frac{1}{5}\{4\ 2\ 0\}$ positions (Fig. 2f) are the long-range ordered (LRO) spots [12]. The volume fraction and size of the ordered domains increase with ageing time (Fig. 2d–e). The LRO micro-domains are cuboid shaped with domain boundaries along $\{100\}_{fcc}$, for anti-parallel twins, and $\{110\}_{fcc}$, for perpendicular twin boundaries resulting in a total of six variants. The domain size shows a large scatter, primarily because of their joining up in one direction. On an average, each unit domain has been found to be ∼ 105 nm after 50 h of ageing at 1073 K. The orientation relationship between $D1_a$ phase and parent fcc matrix is described in detail by Banerjee et al. [5] and Hata et al. [7, 8] and is not repeated here.

The high-resolution TEM images recorded for the alloy aged at 1073 K for 4 h show a sharp interface indicating that the ordering transition at 1073 K is a first-order transition (Fig. 3a–b) and the ordered domains grow by the conventional nucleation and growth process.

3.1.2 Microstructure-property correlations

The Vicker's microhardness was measured at different ageing temperatures to observe the effect of ordered domain formation on alloy strength (Fig. 4). It is evident from the plot that formation of LRO domains in the fcc matrix results in an increase in average microhardness

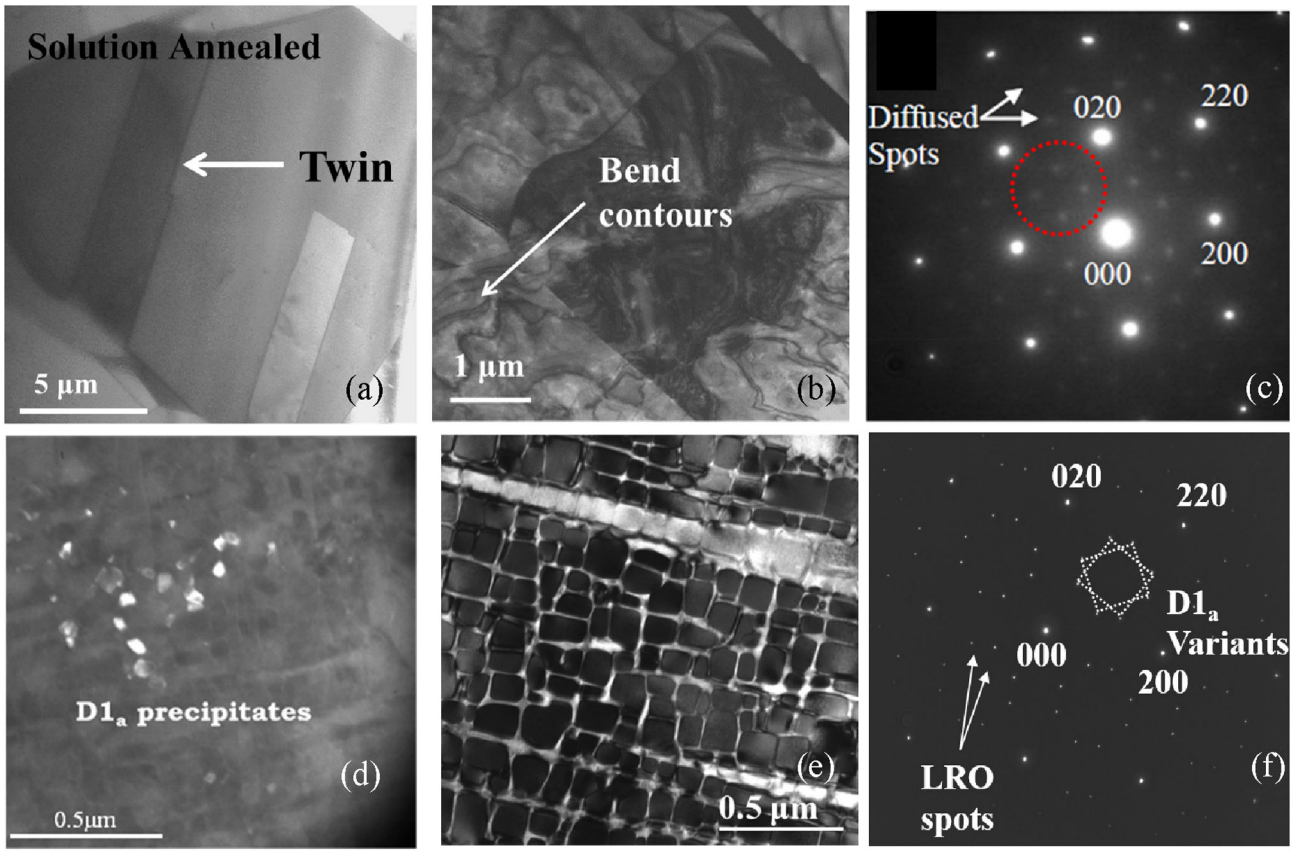

Fig. 2 Bright field image for **a** as-quenched alloy and **b** alloy aged at 873 K for 2 h. **c** SAED pattern along [001] zone axis for the alloy aged at 873 K for 2 h. Bright field micrographs for alloy aged at 973 K for **d** 4 h and **e** 50 h, respectively, and **f** diffraction pattern for the alloy aged at 973 K for 4 h recorded along [001] zone axis

value from 307 (± 10) Vickers hardness number (VHN) for as-quenched Ni-20 at.% Mo alloy to 873 (± 15) VHN for ordered specimens. The increase in hardness is attributed to a substantial increase in the bond strength due to ordering and presence of coherent interface strains between adjacent domains.

3.2 Calculation results

3.2.1 Determination of interaction parameters and ground-state properties

Pair, triplet and quadruplet clusters were generated to efficiently describe the configurational energies of the ordered structures for Ni–Mo system containing upto 10 atoms/unit cell. The ordered ground states of Ni–Mo system, viz. $L1_o$ type—NiMo, Pt_2Mo type -Ni_2Mo, $L1_2$ type -Ni_3Mo, $D1_a$ type -Ni_4Mo have negative formation enthalpies suggesting that the phases are stable at 0 K. Amongst these, equiatomic NiMo ($L1_0$) is the most stable structure in Ni–Mo system as compared to the other configurations since it has the lowest formation energy (− 0.966 eV/atom). The cohesive energies for selected ordered structures (Mo: 0–50 at%) are given in Table 2 and are found to be in concordance with the values reported by Zhou et al. [20].

Amongst the various clusters (as presented in Fig. 5), the magnitude of ECI value is maximum for pair cluster with cluster diameter at 2.47 Å followed by the one with diameter 3.5 Å. The magnitudes of calculated triplet and quadruplet ECIs are lower as compared to pair clusters indicating a good convergence of CE model. A similar observation was made by Banerjee et al. when using the CE formalism on Ni–Mo system with7 atoms/cell [11]. Additionally, it was observed that with an increase in the cluster diameter for each type of cluster, the magnitude of the ECI decreases. This suggests that only the first few NN interactions play a crucial role in the configurational energy of the alloy. From the sign of the normalized ECIs, it is evident that Ni–Mo bonds are preferred as NN along the (110) coordination shell as the normalized ECIs are positive; while Ni–Ni and Mo-Mo bonds are preferred along the second coordination shell for which the ECIs are negative. The ECI value for triplet, as well as quadruplet cluster corresponding to the smallest cluster diameter of 2.47 Å (first NN), is also positive indicating that the

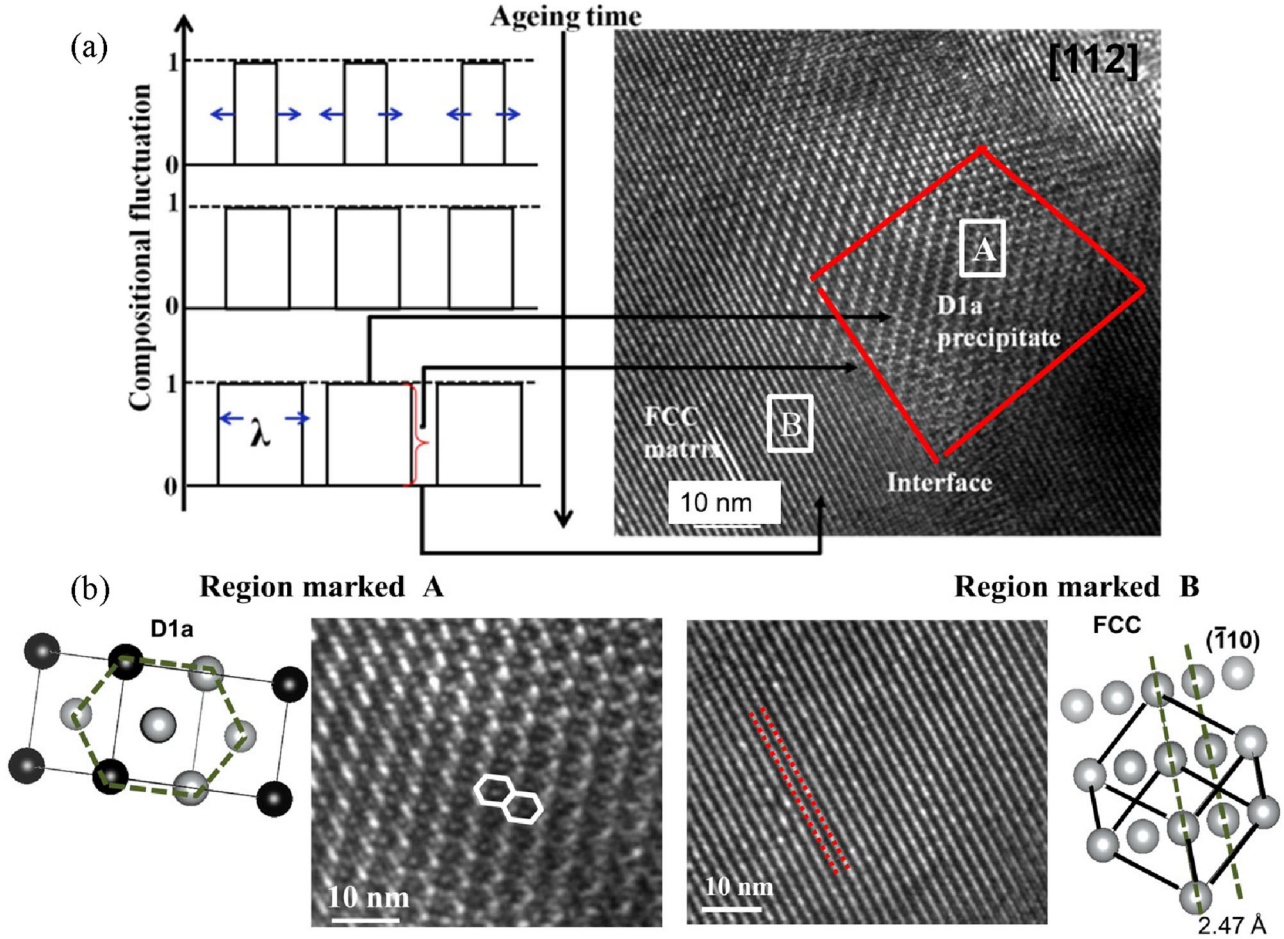

Fig. 3 **a** High-resolution image of Ni_4Mo aged at 1073 K for 4 h along [112] zone axis. The regions are correlated with the schematic showing compositional fluctuations during nucleation and growth process. **b** Crystal projections of regions marked as "A" and "B" in (**a**)

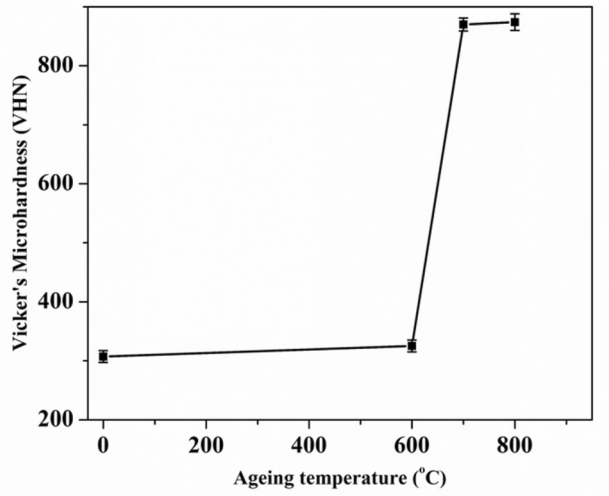

Fig. 4 Vicker's microhardness of the alloy as a function of ageing temperature at constant ageing time of 2 h

multisite interactions also stabilize the ordering tendency. This is in close agreement with the previous hypotheses by Hata et al.[7, 8] and Kulkarni et al.[12]. The detailed comparison of obtained pair and multisite ECIs with the composition-dependent ECIs obtained via cluster variation method are discussed at length by Banerjee et. al. [11] and are not repeated here.

3.2.2 Evaluation of Warren Cowley parameters

The WC parameters, α_l (where l denotes the coordination shell considered), for ordered Ni_4Mo phase with $D1_a$ structure and Pt_2Mo type Ni_2Mo phase at 300 K were calculated from equilibrium correlation functions using Eq. 3 where $c = 0.2$ for Ni_4Mo and 0.33 for Ni_2Mo. The sign of α determines whether the atoms prefer to order ($\alpha < 0$) or cluster ($\alpha > 0$). For Ni_4Mo, the negative values of $\alpha(1)$, $\alpha(4)$ shells suggest that Ni prefers Mo as its first and fourth NN; while the positive values of $\alpha(2)$ and $\alpha(3)$ suggest that Ni prefers Ni as its second and third NN (Fig. 6a). Similarly, for ordered Ni_2Mo phase (Fig. 6b), the negative values of α for $\alpha(1)$ and $\alpha(4)$ shell suggests that Ni prefers Mo as its first and fourth NN; while the positive

Table 2 Cohesive energies of various ordered Ni–Mo structures evaluated at 0 K using DFT-GGA calculations

System	Cohesive energies (eV/atom)	
	Present study	Ref. 20
Ni fcc	− 5.519	− 5.4827
Mo bcc	− 10.8271	− 9.849
Mo fcc	− 10.417	− 8.041
NiMo	− 7.466	− 7.400
Ni_4Mo	− 6.683	− 6.629

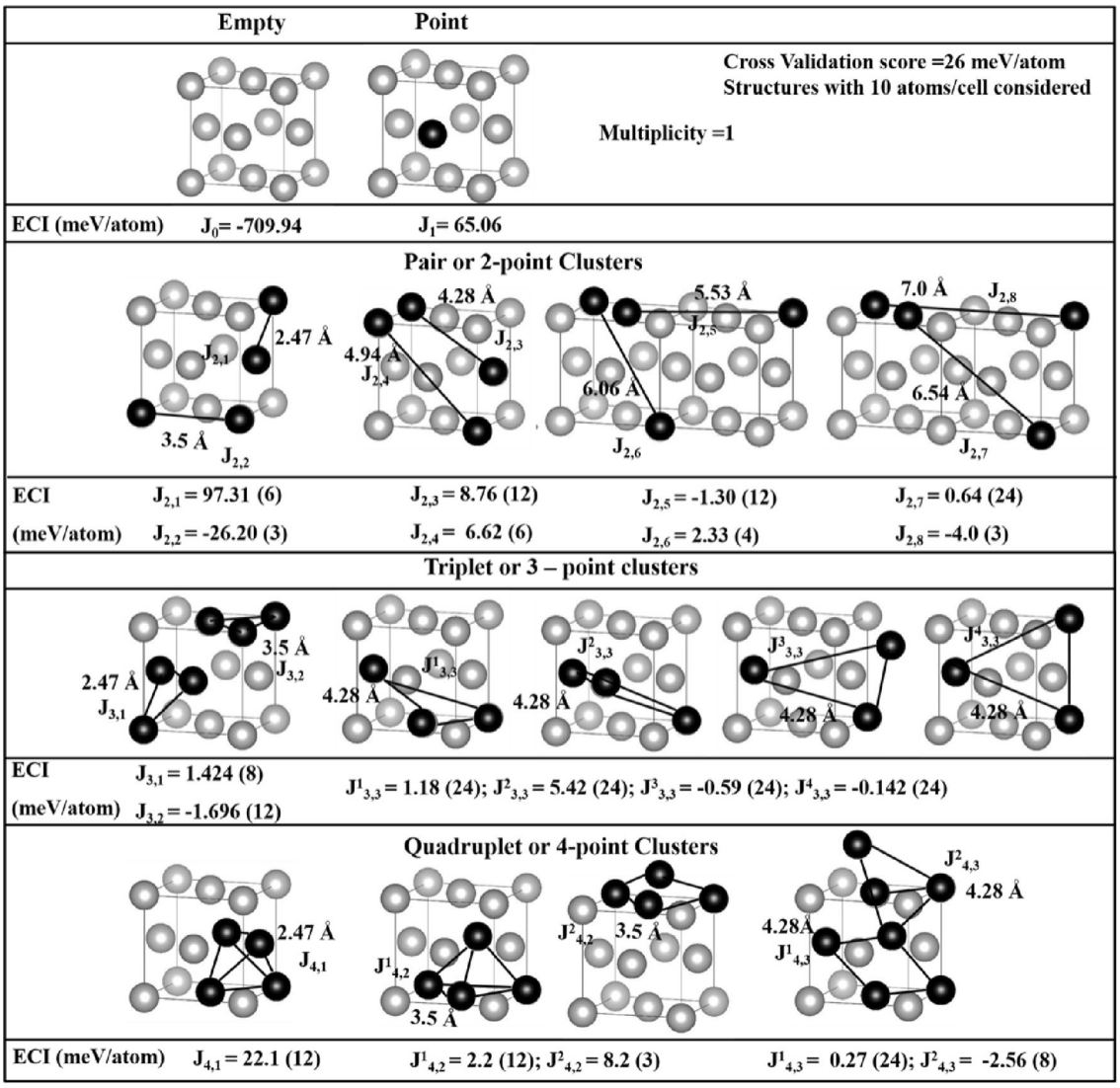

Fig. 5 The truncated set of clusters generated for Ni–Mo system considering 10 atoms/cell. The $J_{n,i}$ are the ECIs where 'n' denotes the type of cluster (0 = empty, 1 = point, 2 = pair and so on); while *i* denotes the ith nearest neighbour

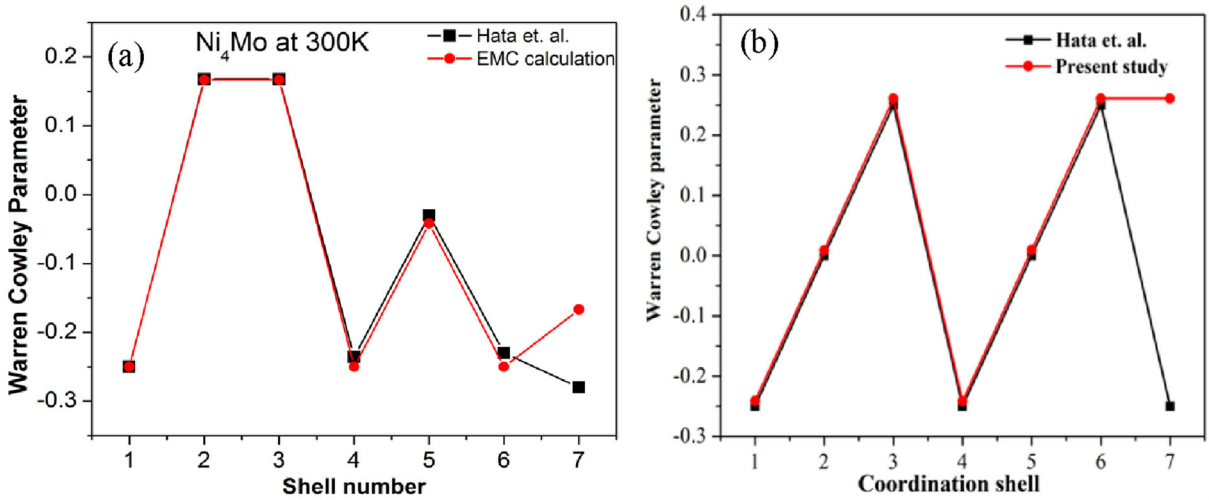

Fig. 6 Warren Cowley parameters for **a** $D1_a$ and **b** Pt_2Mo structures at 300 K

values of α(3) and α(6) suggest that Ni prefers Ni as its third and sixth NN. The evaluated WC parameters match closely with the parameters calculated by Hata et al. [7, 8].

3.2.3 Modelling of order–disorder phase transformations in Ni–20 at% Mo alloy

From the Monte Carlo simulations, at ~ 1000 K, the WC parameters for all the seven coordination shells for Ni_4Mo approach values are close to zero, which correspond to the disordered fcc phase with no preference for either like or unlike atom indicating the initiation of order ($D1_a$) to disordered (fcc) phase transition at ~ 1000 K (Fig. 7a). Similarly, the LRO parameter (η) (Fig. 7b) is found to change from 0.99 at 300 K to 0.72 at 1000 K, indicating the tendency of disordering at a temperature higher than 1000 K. The estimated value of Gibbs free energy for the ordered Ni_4Mo ($D1_a$ structure) phase changes from − 0.62 eV at 300 K to − 0.39 eV at 1000 K. On extrapolation of η in Fig. 7b, the temperature at which is $\eta = 0$ is found to be 1155 K. It is to be noted that the order–disorder transition in Ni_4Mo alloy has been experimentally found to occur at 1140 K [4]; while the calculations show that the transition can occur at a lower temperature. This is owing to the fact that the vibrational (and possibly the kinetic) effects are neglected in the calculations.

4 Summary

The important findings of the present study are summarized as follows:

(a) The as-quenched structure of binary Ni-20 at.% Mo alloy correspond to a SRO structure characterized by

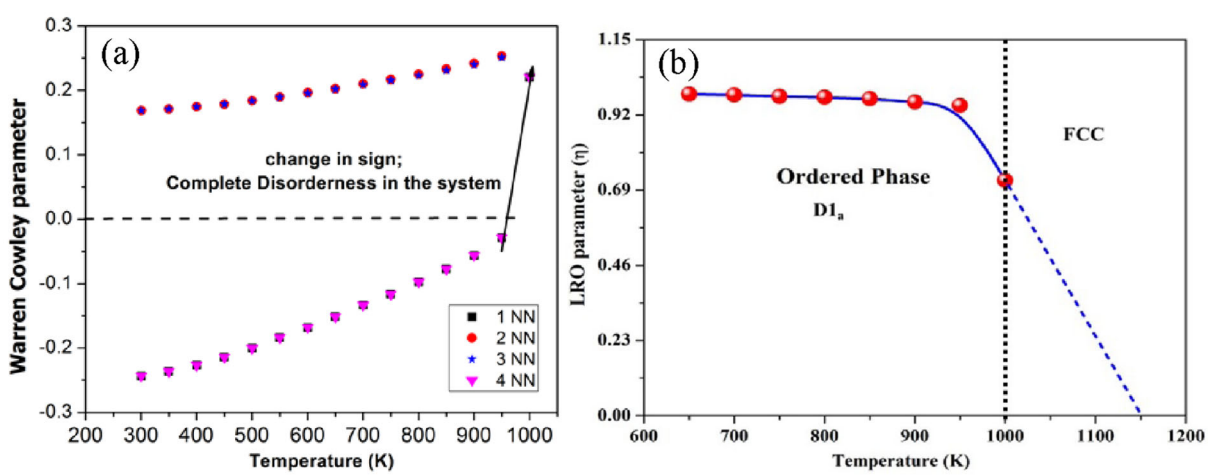

Fig. 7 Variation in **a** SRO parameters for the first four coordination shell **b** LRO parameter as a function of temperature

diffuse {1 ½ 0} reflections in the SAED pattern; while the LRO structure of the aged (at a temperature below the reported ordering temperature) alloy is described by the $D1_a$ structure which grows coherently with the fcc matrix via nucleation and growth process.

(b) Evaluation of the ordering tendency of the alloy was rationalized with respect to the ECIs calculated by CE approach. The evaluated pair interaction parameters (related to pair interaction energies) indicate a clear preference for unlike atoms at first coordination shell which facilitates the formation of both SRO and LRO structures. The multisite interaction parameters for the Ni–Mo alloy have been evaluated for the first time and both the triplet, as well as the quadruplet, interactions have been observed to stabilize the ordering tendency.

(c) From the Monte Carlo simulations, the order–disorder phase transition temperature (T_c), high temperature WC parameters up to fourth NN distance and LRO parameter for Ni_4Mo system have been evaluated. The value of T_c has been found to match closely with the transition temperature reported from experimental investigations.

It is thus established that the diffraction experiments in conjunction with the CE-based calculations can be applied with reasonable accuracy to demonstrate the order–disorder phase transformation behaviour of the Ni–Mo alloys.

5 Declaration

6 Conflict of interest

None.

Acknowledgements The present study was funded by the Department of Atomic Energy, Government of India. The present investigation was carried out as a part of PhD work for one of the authors (RHB) under the supervision of Late Dr. Srikumar Banerjee. The authors are extremely grateful to Dr. Srikumar Banerjee for his valuable discussions and supervision during this study. The authors also thank Dr. V. Kain for his keen interest in this study.

References

1. Song M, Yang Y, Wang M, Kuang W, Lear C R, and Was G S, *Acta Mater* **156** (2018) 446.
2. Arya A, Kulkarni U D, Dey G K, and Banerjee S, *Metall Mater Trans* **39A** (2008) 1623.
3. Arya A, Dey G K, Vasudevan V K, and Banerjee S, *Acta Mater* **50** (2002) 3301.
4. Verma A, Singh JB, Wanderka N, and Chakravartty J K, *Acta Mater*, **96** (2015) 366.
5. Banerjee S, Urban K, and Wilkens M, *Acta Metall* **32** (1984) 299.
6. Arya A, Banerjee S, Das GP, Dasgupta IN, Saha-Dasgupta T, and Mookerjee A, *Acta Mater*, **49** (2001) 3575.
7. Hata S, Matsumura S, Kuwano N, and Oki K, *Acta Mater*, **46** (1998) 881.
8. Hata S, Fujita H, CG S, Matsumura S, Kuwano N, and Oki K, *Mater Trans JIM* **19** (1998) 133.
9. Arya A, Das G P, Banerjee S, and Patni M J, *J Phys Condens Matter* **10** (1998) 8459.
10. Wu Q, He B, Song T, Gao J, and Shi S, *Comp Mater Sci* **125** (2016) 243.
11. Banerjee R H, Arya A, and Banerjee S, *AIP Conf Proceed* **1942** (2018) 090016, pp 4.
12. Kulkarni UD, *Acta Mater* **52** (2004) 2721.
13. Banerjee RH, Arya A, Donthula H, Nayak C, Bhattacharya D, and Banerjee S, *Acta Mater*, 219 (2021) 117263, pp 12.
14. van de Walle A, Asta M, and Ceder G, *Calphad* **26** (2002) 539.
15. Kresse G, Marsman M, and Furthmüller J, VASP the guide, http://cms.mpi.Univie. ac.at/vasp/.
16. Perdew J P, Burke K, and Ernzerhof M, *Phys Rev Lett* **77** (1996) 3865.
17. Monkhorst H J, and Pack J D, *Phys Rev B* **13** (1976) 5188.
18. Hoffmann M, Marmodoro A, Ernst A, Hergert W, Dahl J, Lång J, Laukkanen P, Punkkinen M P, Kokko K, *J Phys Condens Matter* **28** (2016) 305501.
19. Xu X, and Jiang H, *J Chem Phys* **150** (2019) 034102, pp 11.
20. Zhou S H, Wang Y, Jiang C, Zhu J Z, Chen L Q, and Liu Z K, *Mater Sci Engg A* **397** (2005) 288.

Publisher's Note Springer Nature remains neutral with regard to jurisdictional claims in published maps and institutional affiliations.